Magazine of Civil Engineering

ISSN 2712-8172

journal homepage: http://engstroy.spbstu.ru/

Research article

UDC 691.3

DOI: 10.34910/MCE.138.10

Ternary blended concrete synergy of mineral admixtures

A. Kumar[1], ***V. Kumar***[1], ***S. Kumar***[1], ***A.K. Orlov***[2], ***S. Dixit***[3] ✉

[1] *National Institute of Technology, Jamshedpur, India*

[2] *National Research University "Moscow State University of Civil Engineering", Moscow, Russian Federation*

[3] *Centre of Research Impact and Outcome, Chitkara University, Rajpura, Punjab, India*

✉ *sauravarambol@gmail.com*

Keywords: ternary blended concrete, workability, compressive strength, synergy, efficiency factor

Abstract. Concrete that uses supplementary mineral admixtures offers a route to reduce clinker use while maintaining performance, yet the combined action of multiple admixtures in one binder remains uncertain. The potential for synergy among metakaolin (MK), fly ash (FA), and rice husk ash (RHA) has been emphasized in prior work as a means to enhance packing and pozzolanic reaction. The gap addressed here is the absence of a practical way to quantify the combined efficiency of MK–FA–RHA and to predict strength across a broad range of ternary blends. The objective is to evaluate ternary MK–FA–RHA concretes and to derive synergy/efficiency-based equations to predict compressive strength and to correlate it with split tensile and flexural strength. An M25 mixture with water/binder 0.45 and 39 combinations (MK 6–8 %, FA 5–15 %, RHA 5–20 %) was produced; slump, compressive strength (7, 28, 56 days), split tensile and flexural strength were measured using IS:516 specimens (150 mm cubes, 75×150 mm cylinders, 100×100×500 mm beams). Workability decreased with increasing fines: at MK 7 %, the slump fell from 188 mm to ≤100 mm as FA and RHA rose, and reached 35 mm at MK 8 %, FA 10 %, and RHA 20 %. Strength responses showed that 8 % MK alone raised 28- and 56-day compressive strength to 37.24 and 41.76 MPa (vs 34.87 and 38.87 MPa for the control), while RHA ≥15 % produced 15–30 % lower 28-day strength; the best ternary blend across all mixes was 8 % MK + 10 % FA + 10 % RHA. Regression-based equations that incorporated a synergy factor accurately reproduced compressive strength, with most errors within 0–10 %, and yielded R^2 values of 0.73–0.82. Companion correlations predicted split tensile and flexural strengths from compressive strength. These findings suggest that MK 8 % with FA and RHA at 10 % each balances clinker reduction and strength, although high RHA contents require rheology control to avoid consolidation-limited results. Future work is recommended on durability mechanisms and admixture optimization to extend the predictive framework.

Citation: Kumar, A., Kumar, V., Kumar, S., Orlov, A.K., Dixit, S. Ternary blended concrete synergy of mineral admixtures. Magazine of Civil Engineering. 2025. 18(6). Article no. 13810. DOI: 10.34910/MCE.138.10

1. Introduction

Concrete production had relied heavily on ordinary Portland cement (OPC), which carried both environmental and performance costs when mixtures were pushed to meet durability targets in aggressive exposures. Supplementary mineral admixtures had offered a practical path to reduce clinker content while sustaining mechanical and transport properties, and construction practice had increasingly combined more than one admixture in the same binder. The combined use of metakaolin (MK), fly ash (FA), and rice husk ash (RHA) was expected to densify the paste through particle packing and extend hydration through pozzolanic reactions that continued beyond the early ages [1]. The concept of synergy among mineral

admixtures had been central to this promise, because the interaction of several fine powders had produced effects greater than the arithmetic sum of their individual actions. The literature had captured this idea and had described how very fine MK particles and even finer FA and RHA particles had filled voids and refined the matrix, thereby enhancing strength and durability metrics when the mixture had been proportioned appropriately. The efficiency factor framework for pozzolans had also been advanced, with prior work defining k-values to express the cement-equivalent contribution of a single additive, and several authors adopting or extending Bolomey's strength relation to estimate the binder response as replacement levels changed [2]. Despite this foundation, applied mixture design still lacked a clear way to express the combined efficiency of several admixtures acting simultaneously in concrete, and designers often treated the separate k-values independently, even when the paste contained more than one additive.

The gap that motivated the present work lay in the absence of a practical, data-supported framework that quantified the joint efficiency of MK, FA, and RHA and predicted compressive strength for a wide range of ternary blends using a single set of equations. Prior research had typically addressed one admixture at a time or reported ternary results without developing those observations into a predictive tool that mixture designers could use directly [3]. The literature had indicated the importance of this step because efficiency-based accounting had allowed for cement reductions by crediting the equivalent cement content of each additive; yet, a ternary binder had demanded a means to capture the synergy that arose from concurrent physical filling and pozzolanic reactions. The novelty of this work lay in the explicit derivation of strength equations for MK–FA–RHA concrete using Bolomey's relation as the backbone, augmented with an efficiency construct that had represented the combined action of the three powders rather than treating them as isolated substitutions. It also lay in the development of companion correlations that linked compressive strength to split tensile and flexural strength, so that the dataset supported multiple performance predictions from a single measured variable [4].

This work was executed on a broad experimental matrix that covered realistic dosing ranges for practical concretes. The mixture set had included concretes, in which MK had been held at 6, 7, or 8 %, and where FA and RHA had been varied from low to relatively high contents, producing a family of mixes that spanned 39 combinations. Evidence within the dataset showed MK at 6 % with FA and RHA stepped at 5, 10, 15, and 20 %, as well as MK at 8 % paired with the same FA and RHA increments. The ranges captured both moderate and fine-rich pastes [5]. Fresh properties had been recorded through slump, and mechanical properties had been measured at 7, 28, and 56 days so that early and later age behavior had been represented. This design allowed for a direct examination of how additional fines and pozzolanic silica influenced workability, consolidation tendencies, and strength development. Slump observations had shown that the fines content had mattered greatly: mixtures with high RHA and elevated FA at constant MK had exhibited steep reductions in slump, with severe combinations yielding very low values indicative of high yield stress, admixture adsorption, and limited free water for lubrication. Guidance on keeping RHA at or below 10 % when FA had been 5 % or higher had emerged from the data to avoid consolidation defects during strength testing [6].

Responses within this matrix highlighted two patterns essential to the motivation for a predictive framework. First, MK, by itself, had elevated 28- and 56-day strength when dosed at 8 %, confirming the beneficial filler-pozzolanic role of this highly reactive aluminosilicate. Second, the ternary combinations exhibited a clear optimum in the vicinity of 10 % FA and 10 % RHA when MK was 8 %, with that mixture delivering the strongest performance among all 39 combinations. Where RHA exceeded 10 %, the dataset showed persistent reductions in strength that aligned with the mechanistic expectation of increased specific surface, dilution of clinker and greater admixture demand [7]. Yet at about 10 % RHA, gains between 28 and 56 days had been marked, consistent with sustained pozzolanic consumption of portlandite and secondary C–S–H formation that had densified the matrix as curing had progressed. These observations had reinforced the need for a model that had combined physical packing and chemical reaction effects into a single efficiency term applicable to ternary systems [8].

The research gap therefore lay not just in missing data but in the lack of a design-level tool that had transformed such data into equations ready for proportioning work. While single-admixture k-values had existed, they had not accounted for the mutual influence that three powders had exerted on water demand, dispersion, and reaction kinetics when they had been blended in one binder [9]. The novelty statement for the present work captured two contributions. First, the work proposed an efficiency representation that was calibrated directly from the ternary dataset, allowing designers to estimate compressive strength from a chosen set of replacement levels using Bolomey's equation, augmented to include the combined effect of MK, FA, and RHA. Second, the work had produced empirical links between tensile and flexural strength, allowing one model to serve multiple mechanical performance needs without requiring additional calibration data. This pairing of a ternary efficiency construct with cross-property correlations had not been presented for MK–FA–RHA concretes in prior works. The scope of the 39-mix matrix allowed the model to be grounded in a wide range of replacement combinations [10].

The purpose of the investigation was stated accordingly. The work had aimed to evaluate the performance of ternary concretes made with MK, FA, and RHA across practical replacement levels, to document the fresh and hardened responses at relevant curing ages, and to derive a synergy-aware efficiency formulation integrated with Bolomey's strength relation that had predicted compressive strength across the matrix [11]. A second aim was to establish regression-based correlations that connected compressive strength to split tensile and flexural strength, thereby supporting their use in practice when only one property had been readily measured. The introduction had grounded the research questions in the need for clinker reduction through intelligent use of waste-derived mineral admixtures while preserving structural performance, had framed the missing predictive capability for ternary systems as a barrier to adoption and had justified the program design by showing how the experimental matrix had captured both the beneficial and the adverse regimes identified by slump and strength outcomes in the research. The objective of the work was therefore to generate and calibrate an efficiency-based predictive framework for MK–FA–RHA ternary concrete, using a comprehensive set of mixtures and tests to quantify workability and strength at three ages, and to provide correlations to additional strength measures so that the resulting equations had served as practical design aids grounded in the data presented in the research [12].

2. Materials and Methods

2.1. Materials Used

Cement as a binding material

The cement employed was OPC 43 grade, conforming to the Indian standard IS 8112 (1989). The binder material's physical properties are as follows:

- the fineness modulus is 2.74;
- the normal consistency is 29 %;
- the specific gravity is 3.15;
- the initial setting time is 90 minutes;
- the ultimate setting time is 220 minutes.

The strength measurements at 3, 28, and 56 days were recorded as 32.5, 42.5, and 56.5 MPa, respectively.

The chemical parameters of OPC are as follows:

- lime saturation factor: 0.85;
- alumina to iron oxide ratio: 1.13 %;
- insoluble residue: 1.69 %;
- magnesium oxide: 3.02 %;
- loss on ignition: 2.43 %;
- total chloride: 0.018 %.

2.2. Aggregate

The fine aggregate utilized in this study was sourced locally and conformed to the IS 383 (1970) Zone II grading specifications. A sieve analysis was conducted to assess the fineness modulus, specific gravity and water absorption of the fine aggregate. The results were as follows:

- the fineness modulus was 2.75;
- the specific gravity was 2.62;
- the water absorption was 1.3 %.

Alternatively, crushed stone measuring 20 and 12.5 mm was utilized. The fineness modulus, specific gravity and water absorption of 20 mm coarse aggregate was 8.22, 2.63, and 0.42 %, respectively. Identical values to 12.5 mm coarse aggregate: 7.7, 2.73, and 0.54 %.

Water reducing agent

The experiment utilized Auramix 400, a high-range water-reducing admixture produced by the FOSROC brand. This product adheres to the requirements stated in IS 9103 (1999) (2007). To improve the workability of the concrete, a consistent addition of 0.8% (by weight of cement) was incorporated as an enhancement. Nonetheless, potable water was employed for the casting and curing of all concrete specimens. A water-to-binder (w/b) ratio of 0.45 has been used for the concrete mixture design.

Supplementary cementitious materials

This experimental study employed three distinct supplementary cementitious materials: MK, FA, and RHA. This article presents a summary of the physical and chemical characteristics of various admixtures, as detailed in Tables 1 and 2.

Table 1. Physical property of mineral admixtures.

Physical Properties	Metakaolin	Fly Ash	Rice Husk Ash
Physical State	Micronized Powder	Powder Form	Powder
Odor	Odorless	Odorless	Odorless
Appearance	White Color Powder	Grey White Powder	Grey/off White Powder
Color	White	Grey	Off White
Pack Density	0.5 gm/cc	0.9 gm/cc	9.94 gm/cc
Bulk Density (Loose)	–	–	0.37 gm/cc
PH of 5 % Solution	–	–	7.3
Specific Gravity	2.64	2.10	2.26
Water Absorption	66.80 ml/100 gm	58.60 ml/100 gm	0.12 %
Oil Absorption	64 ml/100 gm	–	97.70 %

Table 2. Chemical properties of mineral admixtures.

Chemical Properties	Metakaolin	Fly Ash	Rice Husk Ash
Silica (SiO_2)	52.86 %	58.72 %	88.90 %
Alumina (Al_2O_3)	44.10 %	42.25 %	2.60 %
Ferric Oxide (Fe_2O_3)	0.45 %	4.6 %	2.23 %
Titanium Oxide (TiO_2)	0.36 %	0.56 %	–
Calcium Oxide (CaO)	0.28 %	0.38 %	0.21 %
Magnesium Oxide (MgO)	0.21 %	0.20 %	–
Pottasium Oxide (K_2O)	0.20 %	0.45 %	0.33
Sodium Oxide (Na_2O)	0.25 %	0.35 %	0.36
Loss on Ignition	0.85 %	3.2 %	4.03 %

2.3. Methods Adopted

In compliance with IS 10262 (2009), the concrete mixtures were combined using the absolute volume method for the M25 grade of concrete. The components were proportioned according to their relative weights. Each concrete mixture was formulated using cementitious materials with a density of 350 kg/m^3, a water-to-cementitious materials ratio of 0.45 and a coarse aggregate-to-total aggregate ratio of 0.60 during manufacture. The application of a specific quantity of superplasticizer aimed to achieve the desired workability by facilitating a slump value adjustment within the range of 100±25 mm. M0 refers to the control mix composed solely of OPC. The classification system categorizes the total combinations of ternary blended concrete mixtures into three distinct categories:

1. Group I: The specimens in this category were formulated by substituting 6–41 % of the cement with 6 % MK, 5–15 % FA, and 5–20 % RHA. The specimens are designated as M1 through M13.
2. Group II: The specimens in this category were formulated by substituting 7–42 % of the cement with 7 % MK, 5–15 % FA, and 5–20 % RHA. The specimens are designated as M14 through M26.
3. Group III: The specimens in this category were formulated by substituting 8–43 % of the cement with 8 % MK, 5–15 % FA, and 5–20 % RHA. The specimens are designated as M27 through M39.

The volume of one batch was determined to be 0.045 m^3, factoring in a 20 % wastage. Table 3 presents the substitution thresholds for various waste products, while Table 4 outlines the quantities of distinct components used in different mixes. Fig. 1 illustrates a series of concrete examples submerged in a water tank for curing purposes [13].

Table 3. Details of replacement levels for ternary cement concrete.

Mix [M]	Materials			
	OPC (%)	MK (%)	FA (%)	RHA (%)
M0	100	0	0	0
M1	94	6	0	0
M2	84	6	5	5
M3	79	6	5	10
M4	74	6	5	15
M5	69	6	5	20
M6	79	6	10	5
M7	74	6	10	10
M8	69	6	10	15
M9	64	6	10	20
M10	74	6	15	5
M11	69	6	15	10
M12	64	6	15	15
M13	59	6	15	20
M14	93	7	0	0
M15	83	7	5	5
M16	78	7	5	10
M17	73	7	5	15
M18	68	7	5	20
M19	78	7	10	5
M20	73	7	10	10
M21	68	7	10	15
M22	63	7	10	20
M23	73	7	15	5
M24	68	7	15	10
M25	63	7	15	15
M26	58	7	15	20
M27	92	8	0	0
M28	82	8	5	5
M29	77	8	5	10
M30	72	8	5	15
M31	67	8	5	20
M32	77	8	10	5
M33	72	8	10	10
M34	67	8	10	15
M35	62	8	10	20
M36	72	8	15	5
M37	67	8	15	10
M38	62	8	15	15
M39	57	8	15	20

Table 4. Quantities of several ingredients for different mixes per unit volume (kg/m³).

Mix [M]	Materials (kg)				FA (kg)	CA (kg)	
	OPC	MK	FA	RHA		12.5 mm	20 mm
M0	350	0	0	0	771.31	481.81	687.33
M1	329	21	0	0	769.94	480.95	686.11
M2	294	21	17.5	17.5	764.68	477.67	681.43
M3	276.5	21	17.5	35	762.35	476.21	679.35
M4	259	21	17.5	52.5	760.02	474.76	677.27
M5	241.5	21	17.5	70	757.68	473.30	675.19
M6	276.5	21	35	17.5	761.76	475.85	678.82
M7	259	21	35	35	759.43	474.39	676.74
M8	241.5	21	35	52.5	757.09	472.93	674.66
M9	224	21	35	70	754.76	471.47	672.59
M10	259	21	52.5	17.5	758.84	474.02	676.22
M11	241.5	21	52.5	35	756.51	472.56	674.14
M12	224	21	52.5	52.5	754.17	471.11	672.06
M13	206.5	21	52.5	70	751.84	469.65	669.98
M14	325.5	24.5	0	0	769.71	480.81	685.91
M15	290.5	24.5	17.5	17.5	764.46	477.53	681.22
M16	273	24.5	17.5	35	762.12	476.07	679.14
M17	255.5	24.5	17.5	52.5	759.79	474.61	677.06
M18	238	24.5	17.5	70	757.45	473.15	674.99
M19	273	24.5	35	17.5	761.53	475.70	678.62
M20	255.5	24.5	35	35	759.20	474.25	676.54
M21	238	24.5	35	52.5	756.87	472.79	674.46
M22	220.5	24.5	35	70	754.53	471.33	672.38
M23	255.5	24.5	52.5	17.5	758.61	473.88	676.02
M24	238	24.5	52.5	35	756.28	472.42	673.94
M25	220.5	24.5	52.5	52.5	753.94	470.96	671.86
M26	203	24.5	52.5	70	751.61	469.50	669.78
M27	322	28	0	0	769.48	480.67	685.70
M28	287	28	17.5	17.5	764.23	477.39	681.02
M29	269.5	28	17.5	35	761.89	475.93	678.94
M30	252	28	17.5	52.5	759.56	474.47	676.86
M31	234.5	28	17.5	70	757.23	473.01	674.78
M32	269.5	28	35	17.5	761.30	475.56	678.42
M33	252	28	35	35	758.97	474.10	676.34
M34	234.5	28	35	52.5	756.64	472.64	674.26
M35	217	28	35	70	754.30	471.19	672.18
M36	252	28	52.5	17.5	758.38	437.37	675.81
M37	234.5	28	52.5	35	756.05	472.28	673.73
M38	217	28	52.5	52.5	753.72	470.82	671.65
M39	199.5	28	52.5	70	751.38	469.36	669.57

Note: Quantity of super plasticizer was calculated as 2.8 kg/m^3 for all mixes.

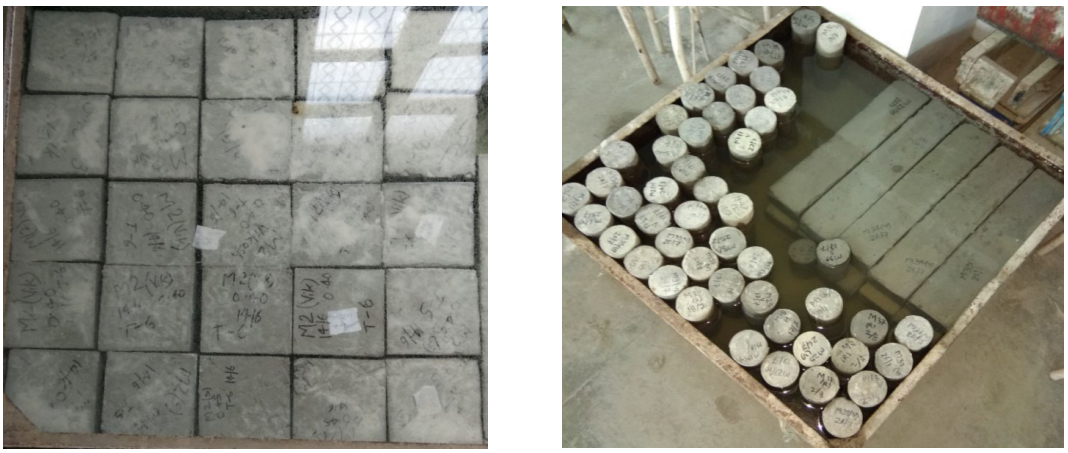

Figure 1. A set of concrete specimens prepared for each mix.

2.4. Testing of Concrete Specimens

The workability of concrete refers to its ability to undergo efficient mixing, placement, consolidation, and finishing. The quality of freshly mixed concrete significantly influences its ease and homogeneity during these operations. The workability of concrete was evaluated utilizing a slump cone measuring 100×200×300 mm, in compliance with the IS 1199 (1959) standard. The slump test is performed between batches to evaluate the uniform quality of concrete throughout the construction process.

The compressive strength of a material denotes the greatest force it can endure prior to complete failure. The compressive strength was calculated by dividing the failure force by the cross-sectional area that bore the load. The compressive strength of 150 mm cube specimens was assessed in accordance with IS 516 (1959) using a digital compression testing machine after 7, 28, and 56 days of curing.

The split tensile strength of 75×150 mm cylinder specimens was measured in accordance with IS 516 (1959). The split tensile strength was determined by applying the formula $T = 2 \times P / (\text{ПП} \times D \times L)$. However, the flexural strength was assessed using beam specimens of 100×100×500 mm, in accordance with IS 516 (1959), which is commonly referred to as four-point loading. The flexure strength was determined by applying the formula

$$F_b = PL / bd^2,$$

where F_b is the flexure strength; P is the applied load; L is the length; b is the width; d is the thickness of the material.

This calculation was used because the shear span is less than 110 mm.

3. Results and Discussions

3.1. Characteristics of Freshly Mixed Concrete

The workability of concrete is typically employed to assess its fresh qualities. Four categories have been established based on the workability findings of the concrete.

1. Group I: Ternary blended concrete produced by replacing 6–8 % of the cement with MK;
2. Group II: Ternary blended concrete produced by replacing 6 % MK, 5–15 % FA, and 5–20 % RHA for the cement in M1, M14, and M27. M2–M13;
3. Group III: Ternary blended concrete produced by replacing 7 % MK, 5–15 % FA, and 5–20 % RHA for the cement, which constitutes 17–42 % of the mixture. M15–M26;
4. Group IV: Ternary blended concrete produced by replacing 8 % MK, 5–15 % FA, and 5–20 % RHA for 18–43 % of cement, specifically M28–M39 [14].

The optimal depiction of these configurations, illustrating diverse category outcomes, can be located in Figs. 2–5.

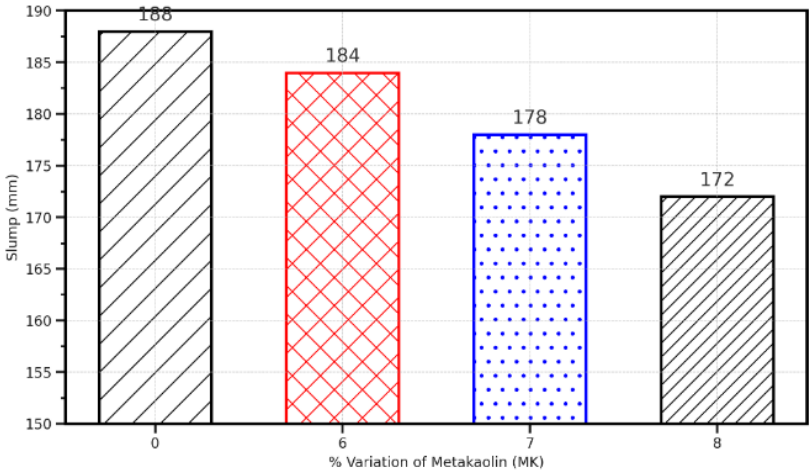

Figure 2. Workability of Group I ternary blended concrete specimens using 6–8 % MK.

Fig. 2 shows the slump response as MK replaces cement from 0 to 8 %. Workability declines steadily: from 188 mm at 0 % MK to 184 mm at 6 % (−4 mm; **−2.1 %**), then to 178 mm at 7 % (**−5.3 %** vs control) and to 172 mm at 8 % (**−8.5 %** vs control). Stepwise losses are modest up to 6 % MK but become more pronounced between 6→7 % (**−3.3 %**) and 7→8 % (**−3.4 %**), indicating a threshold where MK's rheological effects outweigh any dispersion from the superplasticizer. This trend aligns with MK's very high fineness and angular morphology, which increase the specific surface area and water demand; the additional surfaces promote flocculation and inter-particle friction, thereby thickening the paste. MK's early pozzolanic reactivity also scavenges $Ca(OH)_2$ and releases C–S–H nuclei, which stiffen the suspension and reduce the amount of free water available for lubrication. Practically, mixes at 7–8 % MK may require either a higher superplasticizer dose or a slightly lower aggregate packing density to maintain the target slump without increasing the w/b ratio [15]. This matters for strength and durability experiments: inadequate slump compromises compaction, elevating entrapped air, and biasing compressive strength downward, while also increasing sorptivity in permeability tests. To isolate MK's chemical benefits in later tests (e.g., strength, chloride penetration), keep slump constant across mixes by adjusting admixture dosage at fixed w/b; otherwise, differences in mechanical or transport results could be partly rheology-driven rather than true binder chemistry effects. The small −2.1 % slump drop at 6 % MK suggests a workable upper bound for field placement without admixture retuning, whereas ≥7 % MK should be paired with mix-control steps to preserve placement quality [16].

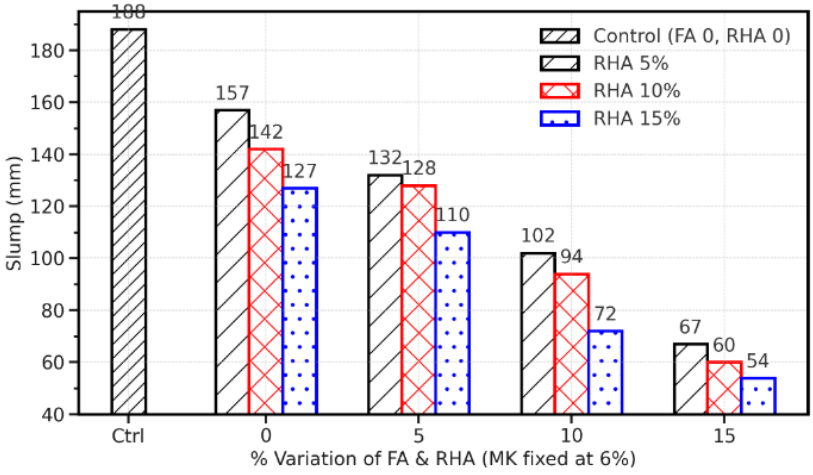

Figure 3. Workability of Group II ternary blended concrete specimens.

Fig. 3 shows the slump response when FA and RHA are varied, while MK is held at 6 %. Relative to the control (188 mm; FA = 0 %, RHA = 0 %), any addition of RHA at FA = 0 % reduces slump: 157 mm at 5 % RHA (−16.5 %), 142 mm at 10 % RHA (−24.5 %), and 127 mm at 15 % RHA (−32.4 %). At fixed RHA, increasing FA sharply lowers workability by roughly the same proportion across all RHA levels: from FA 0→15 %, slump drops 57–58 % (e.g., at RHA 5 %: 157→67 mm, −57.3 %; at RHA 15 %: 127→54 mm, −57.5 %). Raising RHA at fixed FA compounds the loss: at FA = 10 %, going from RHA 5 to 15 % cuts the slump from 102 to 72 mm (−29.4 %), while at FA = 15 %, the step is from 67 to 54 mm (−19.4 %). The most severe combination, FA 15 % + RHA 15 %, yields 54 mm, with a yield stress of 71.3 % versus the control, indicating a paste with high yield stress and poor flow under standard compaction energy. Mechanistically,

the strong slump reductions arise from the very high specific surface of RHA and the fine, reactive MK already present; both increase water demand and adsorb superplasticizer, leaving less free water for lubrication [17]. FA can act as a “ball-bearing”, but at these dosages within a ternary fines-rich system, its benefit is outweighed by increased surface area and potential admixture adsorption (especially for low-lime, high-LOI FA). For subsequent strength or transport tests, these rheology shifts are significant: inadequate slump can raise entrapped air and depress compressive strength while increasing sorptivity. To isolate chemistry-driven performance, keep slump constant across mixes – e.g., cap FA at ≤5 % when RHA ≥ 10 % or increase superplasticizer dosage at fixed w/b – so later durability and strength results are not confounded by compaction differences [18].

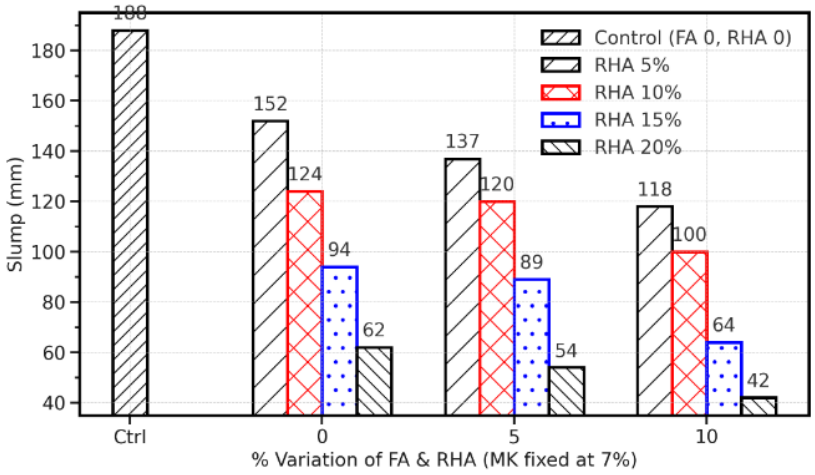

Figure 4. Slump variation of Group III ternary blended concrete mixes.

Fig. 4 illustrates the slump response when FA and RHA are varied, while MK is maintained at a constant 7 % level. Relative to the control (188 mm; FA = 0 %, RHA = 0 %), any RHA addition reduces workability at FA = 0 %: 152 mm at 5 % RHA (−19.1 %), 124 mm at 10 % (−34.0 %), 94 mm at 15 % (−50.0 %), and 62 mm at 20 % (−67.0 %). At FA = 5 %, slump falls to 137, 120, 89, and 54 mm for RHA 5–20 % (−27.1, −36.2, −52.7, and −71.3 % vs. control). At FA = 10 %, the decline is strongest: 118, 100, 64, and 42 mm (−37.2, −46.8, −66.0, and −77.7 %) [19]. The data indicate two compounding effects: (i) increasing RHA sharply increases specific surface area, raising water demand and adsorbing superplasticizer; and (ii) a higher FA level, when combined with reactive MK at 7 %, further elevates fines content and admixture adsorption, leaving less free water to lubricate the paste. Practically, mixes with RHA ≥15 % slip below 100 mm slump, even at FA ≤ 5 %, signaling a risk of poor consolidation unless the admixture is retuned. For FA = 10 % and RHA ≥ 10 %, the slump is 100 mm or lower, which can elevate entrapped air and depress compressive strength, while increasing capillary porosity – factors that will bias results in strength and permeability experiments. To maintain consistent placement while studying MK–FA–RHA chemistry, keep RHA ≤ 10 % when FA ≥ 5 % (slump ≥ 120 mm at FA 5 %, RHA 10 %), or raise superplasticizer dosage/adjust paste volume at fixed w/b. These thresholds help prevent compaction differences from masquerading as binder-performance differences in subsequent mechanical and durability testing [20].

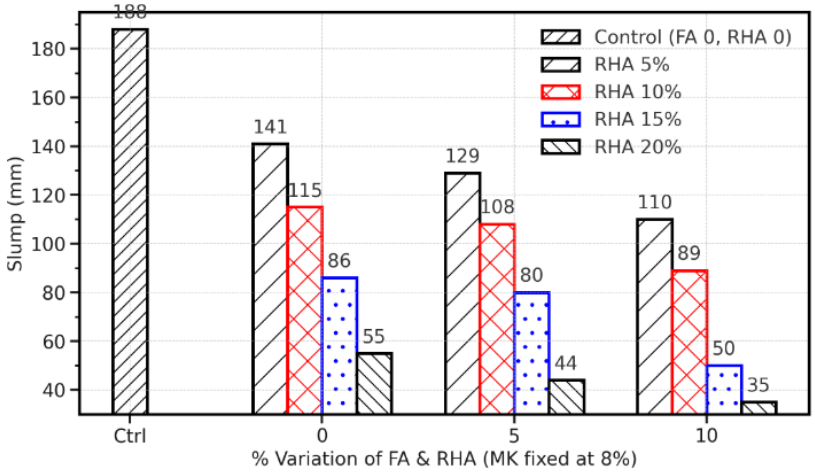

Figure 5. Slump variation of Group IV ternary blended concrete mixes.

Fig. 5 shows the slump response when FA and RHA are varied at a higher MK level (8 %). Relative to the control (188 mm), the FA = 0 % series already exhibits steep losses as RHA increases: 141 mm at 5 % (−25.0 %), 115 mm at 10 % (−38.8 %), 86 mm at 15 % (−54.3 %), and 55 mm at 20 % (−70.7 %). Adding FA further suppresses slump across each RHA level. At RHA=5 %, raising FA from 0→10 % drops slump from 141→110 mm (−22.0 %); at RHA = 10 %, the drop is 115→89 mm (−22.6 %) [21]. The fines-rich combinations are most severe: at RHA = 15 %, FA 0→10 % reduces slump 86→50 mm (−41.9 %), and at RHA = 20 %, 55→35 mm (−36.4 %), culminating in the lowest value (35 mm; −81.4 % vs. control) for FA 10 % + RHA 20 %. Mechanistically, MK at 8 % provides an abundance of reactive, angular particles. Adding porous, ultra-fine RHA increases the specific surface area and admixture adsorption, thereby reducing the water film thickness and elevating the paste yield stress. FA's spherical grains can improve packing, but at these MK–RHA loadings, the net effect is higher surface area and stronger superplasticizer demand, so the "ball-bearing" benefit is overwhelmed. For subsequent mechanical or durability experiments, this rheology shift can confound outcomes, as poor slump risks inadequate consolidation, entrapped air and artificially low compressive strength, with higher sorptivity. To maintain comparable placement, keep RHA ≤ 10 % when FA ≥ 5 % (slump ≥ ~108–115 mm), or re-tune the admixture dosage/paste volume at a fixed w/b ratio. Avoid FA 10 % with RHA ≥ 15 % unless a higher superplasticizer dose is used, as these mixes fall well below 100 mm and are prone to compaction-related scatter [22].

3.2. Hardened Properties of Concrete

Characteristic compressive strength

The specimens were analyzed following 7, 28, and 56 days of water cure. The results have been categorized into three primary groups:

1. Group I consists of ternary blended concrete specimens, wherein 6 % MK, 5–15 % FA, and 5–20 % RHA replace 6–41 % of the cement. The specimens have been assigned the designations M1–M13.
2. Group II consists of ternary blended concrete specimens, in which 7–42 % of the cement is replaced with 7 % MK, 5–15 % FA, and 5–20 % RHA.
3. Group III consists of ternary blended concrete specimens, wherein 8–43 % of the cement is replaced with 8 % MK, 5–15 % FA, and 5–20 % RHA. The specimens are labelled M27–M39.

To elucidate the trend behavior of RHA, each category has been subdivided into multiple forms. This has been accomplished while preserving the equivalent content level for MK and FA. Fig. 6 presents the most precise depiction of the typical values for compressive strength [23].

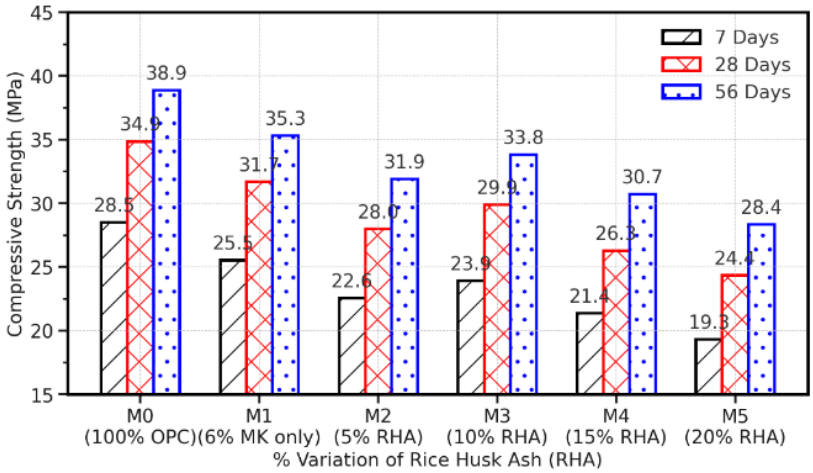

Figure 6. Typical results for compressive strength of Group I ternary blended concrete mixes.

Fig. 6 shows the strength response as RHA rises while MK is fixed at 6 % and FA at 5 %. Against the control M0 (100 % OPC), strengths decrease at every age when RHA is added. At 28 days, M0 reaches 34.9 MPa. With RHA = 5 % (M2) and 10 % (M3), strengths are −19.8 % (27.99 MPa) and −14.2 % (29.91 MPa) relative to M0; higher RHA of 15 and 20 % drop further to −24.6 % (26.28 MPa) and −30.1 % (24.36 MPa). A local optimum appears at RHA = 10 %, which is +6.9 % higher than RHA=5 % and +13.8 % above RHA = 20 % at 28 days. The same pattern holds at 56 days: M0 = 38.9 MPa; M3 = 33.8 MPa (−13.0 % vs M0) yet +6.0 % vs RHA = 5 % and +19.3 % vs RHA = 20 %. Age gains are strong across mixes, highlighting the delayed pozzolanic action of RHA: from 7 to 28 days, strength rises by ~24–26 % (e.g., M3: 23.91 to 29.91 MPa, +25.1 %); from 28 to 56 days, gains are ~13–17 % (M4: 26.28 to 30.73 MPa, +16.9 %). Physically, finely porous RHA consumes $Ca(OH)_2$ to form secondary C–S–H, which explains the

sustained gains from 28 to 56 days; however, excess RHA (>10 %) elevates the specific surface and dilutes the clinker, raising water and superplasticizer demand, which reduces early packing and limits later strength [24]. For downstream durability or modulus tests, the RHA = 10 % condition offers the best balance within this MK–FA matrix, providing higher late-age strength than RHA at 5 % or 15–20 %. Mixes with ≥15 % RHA result in lower compaction quality and higher capillary porosity, without requiring admixture retuning.

Table 3. Compressive strength of Group I ternary blended concrete mixes.

Mix[M]	Blending				Mean Compressive Strength (7 Days)	Mean Compressive Strength (28 Days)	Mean Compressive Strength (56 Days)
	OPC	MK	FA	RHA			
M0	100	0	0	0	28.50	34.87	38.87
M1	94	6	0	0	25.54	31.69	35.32
M2	84	6	5	5	22.58	27.99	31.91
M3	79	6	5	10	23.91	29.91	33.84
M4	74	6	5	15	21.39	26.28	30.73
M5	69	6	5	20	19.32	24.36	28.36
M6	79	6	10	5	25.32	31.17	35.02
M7	74	6	10	10	26.73	32.65	36.58
M8	69	6	10	15	24.65	30.13	34.58
M9	64	6	10	20	22.87	28.50	31.99
M10	74	6	15	5	24.80	30.87	34.73
M11	69	6	15	10	23.76	28.87	33.69
M12	64	6	15	15	21.84	26.87	31.61
M13	59	6	15	20	20.06	25.47	29.69

Nonetheless, the results of the enhancement of compressive strength in Group II ternary blended concrete mixtures, which incorporate the replacement of a designated percentage of cement with 7 % MK, 5 % FA, and 5–20 % RHA, in addition to one control mixture, are illustrated in Fig. 7. The compressive strength values were measured at 27.76, 33.84, and 38.43 MPa after 7, 28, and 56 days of curing, respectively, when ordinary concrete was combined with 7 % MK completely. The readings were recorded following the concrete's curing period of 7, 28, and 56 days. Moreover, the incorporation of 7 % MK, in conjunction with 5 % FA and 5–10 % RHA, results in a reduction in concrete strength relative to the control mix. This phenomenon is noted in several mixtures, notably M15–M18. When concrete is produced by amalgamating varying proportions of RHA with a constant content of 7 % MK and 5 % FA, a significant enhancement in compressive strength has been seen for the concrete containing 10 % RHA (M16) after 7, 28, and 56 days of curing. This pattern resembles that observed in the concrete mixed with merely 7 % MK, as per the M14 formula. Table 4 presents the compressive strength values for Group II ternary blended concrete compositions. The optimal replacement percentage for Group II concrete specimens is 7 % MK, 10 % FA, and 10 % RHA, corresponding to an M20 mix [25].

Table 4. Compressive strength of Group-II ternary blended concrete mixes.

Mix[M]	Blending				Mean Compressive Strength (7 Days)	Mean Compressive Strength (28 Days)	Mean Compressive Strength (56 Days)
	OPC	MK	FA	RHA			
M0	100	0	0	0	28.50	34.87	38.87
M14	93	7	0	0	27.76	33.84	38.43
M15	83	7	5	5	23.61	30.13	34.58
M16	78	7	5	10	25.17	32.21	35.91
M17	73	7	5	15	22.50	29.39	33.24
M18	68	7	5	20	20.06	27.32	31.91
M19	78	7	10	5	26.87	33.54	37.84
M20	73	7	10	10	28.73	36.50	39.47
M21	68	7	10	15	25.69	31.91	35.61
M22	63	7	10	20	23.91	29.84	33.84
M23	73	7	15	5	26.58	33.54	37.76
M24	68	7	15	10	23.91	30.87	34.87
M25	63	7	15	15	23.76	29.99	34.43
M26	58	7	15	20	21.10	28.65	33.10

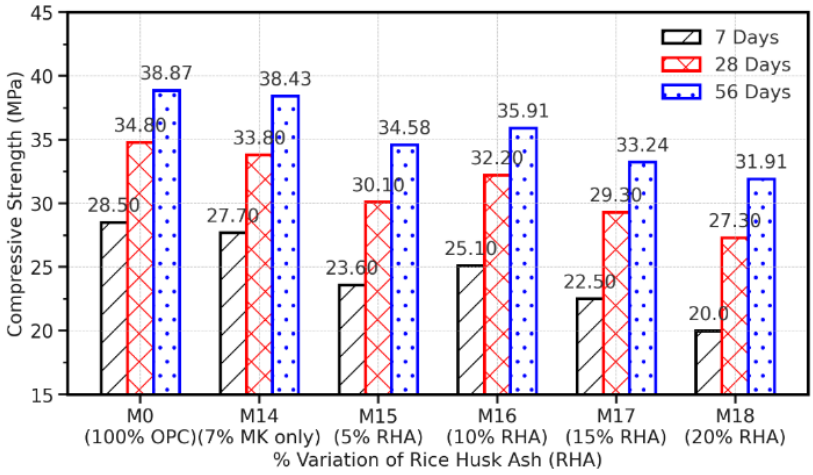

Figure 7. Typical results for compressive strength of Group II ternary blended concrete mixes.

Fig. 7 shows the strength evolution as RHA increases with MK held at 7 % and FA at 5 %. Compared with the 100 % OPC control (M0: 34.8 MPa at 28 days, 38.87 MPa at 56 days), mixes with RHA are lower at both ages, yet 10 % RHA (M16) is consistently the best among the RHA series: 32.2 MPa at 28 days and 35.91 MPa at 56 days −7.5 % (28 d) and −7.6 % (56 d) vs the control, but +7.0 % (28 d) and +3.8 % (56 d) higher than 5 % RHA (M15). At higher RHA, the penalty grows: 15 % RHA (M17) is −15.8 % (28 d) and −14.5 % (56 d) vs control; 20 % RHA (M18) is −21.6 % (28 d) and −17.9 %(56 d). Age gains reveal delayed pozzolanic activity of RHA, which strengthens later, from 28 to 56 days, with strengths rising by ~11–17 % (e.g., M18: +16.9 %, M15: +14.9 %, M16: +11.5 %). Early (7→28 days) gains are larger as RHA increases, reaching +36.5 % for M18, indicating slow early reactivity and progressive secondary C–S–H formation. Mechanistically, modest RHA (~10 %) provides reactive silica and fine filler to densify a paste already enriched with MK, whereas excessive RHA (>10 %) dilutes the clinker, increases surface area, and increases admixture demand, thereby curbing early packing and limiting late strength. For follow-on durability or transport tests, these maturity effects are significant: higher-RHA mixes may appear inferior at 28 days but close the gap by 56 days as pores refine [26]. If the goal is to reduce clinker content while maintaining acceptable strength, 10 % RHA within this MK–FA matrix is a practical upper bound without retuning the admixture or paste volume. A RHA content of ≥15 % should be paired with workability control to avoid compaction-induced scatter in strength and permeability results.

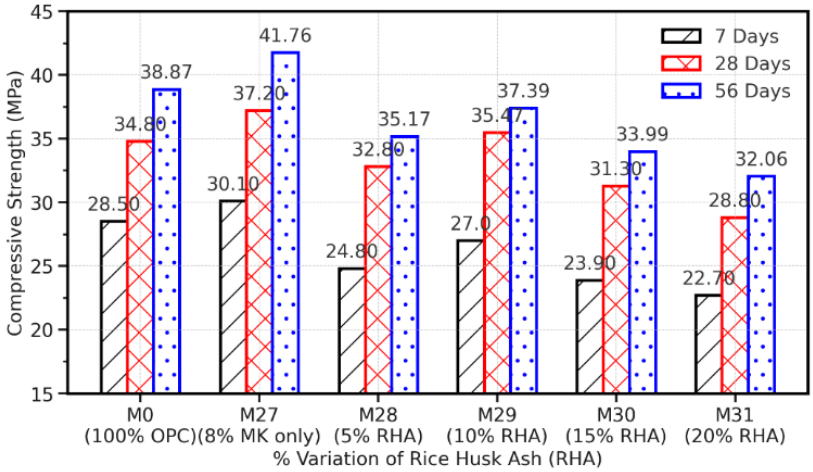

Figure 8. Typical results for compressive strength of Group III ternary blended concrete mixes.

The increase in compressive strength of Group III ternary mixed concrete specimens is illustrated in Fig. 8. This scenario involves substituting 8 % of the cement with MK, 5 % with FA, and 5–20 % with RHA, alongside a control mix. Based on the findings presented in Fig. 8, it can be concluded that incorporating MK into conventional cement concrete enhances the compressive strength of the concrete. For instance, when the concrete is combined with 8 % MK exclusively, the compressive strength values are 30.18, 37.24, and 41.76 MPa after curing for 7, 28, and 56 days, respectively. When the MK concentration reaches 8 %, a noticeable enhancement in compressive strength occurs. Furthermore, when the concrete incorporates 8 % MK alongside 5 % FA and 5–10 % RHA, a decline in strength is observed in other mixtures (namely M28–M31). The reduction in strength is analogous to the decline observed in the control mix. Concrete composed of varying proportions of RHA, combined with a constant 8 % MK and 5 % FA, exhibits a

significant enhancement in compressive strength at 10 % RHA blending (M29) after 7, 28, and 56 days of curing. This observation was made after the concrete had cured for 7, 28, and 56 days. Initially, the compressive strength of the Group III ternary blended concrete specimens was quite low; however, after 56 days of curing, a significant enhancement in strength was noted. Table 5 delineates the specific compressive strength values for ternary mixed concrete mixtures classified under Group III. The optimal replacement proportion for Group III concrete specimens, as well as for all 39 combinations, was established as 8 % MK + 10% FA + 10 % RHA, corresponding to the M33 mix [27].

Table 5. Compressive strength of Group III ternary blended concrete mixes.

Mix[M]	Blending				Mean Compressive Strength (7 Days)	Mean Compressive Strength (28 Days)	Mean Compressive Strength (56 Days)
	OPC	MK	FA	RHA			
M0	100	0	0	0	28.50	34.87	38.87
M27	92	8	0	0	30.18	37.24	41.76
M28	82	8	5	5	24.80	32.80	35.17
M29	77	8	5	10	27.02	35.47	37.39
M30	72	8	5	15	23.91	31.32	33.99
M31	67	8	5	20	22.73	28.80	32.06
M32	77	8	10	5	29.69	37.10	40.80
M33	72	8	10	10	30.87	38.87	42.58
M34	67	8	10	15	27.91	33.99	38.13
M35	62	8	10	20	25.99	30.87	36.36
M36	72	8	15	5	28.80	36.50	39.32
M37	67	8	15	10	26.87	34.43	35.91
M38	62	8	15	15	25.39	31.76	34.87
M39	57	8	15	20	24.21	30.73	34.43

3.3. Flexural Strength

The mean flexural strength of concrete specimens is reported following a 28-day water curing period.

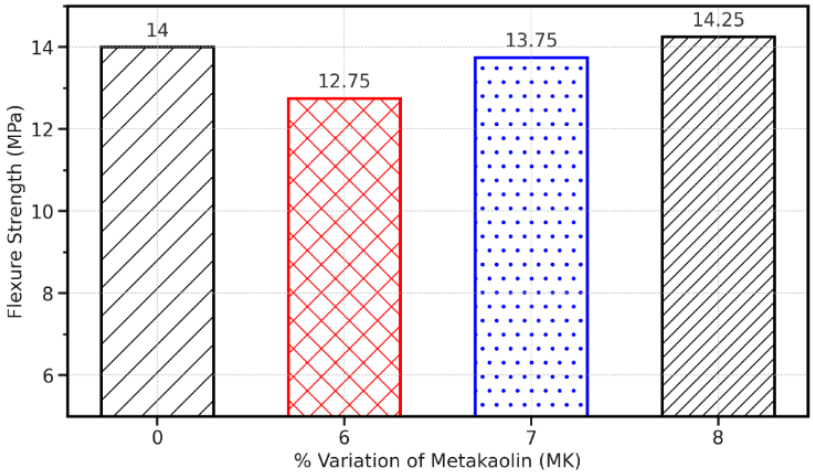

Figure 9. Flexure strength of ternary blended concrete mixes using 6–8 % MK only.

Fig. 9 shows the flexural response as MK replaces cement from 0 to 8 % with no other SCMs. The control (0 % MK) reaches 14.00 MPa. Introducing 6 % MK lowers flexural strength to 12.75 MPa (−8.9 % vs control), likely due to higher water demand and tighter rheology, which reduces fiber bridging at the paste–aggregate interface when the admixture dosage isn't retuned. Raising MK to 7 % recovers strength to 13.75 MPa (+7.8 % vs 6 % MK; −1.8 % vs control), indicating better packing and budding pozzolanic gel that densifies the interfacial transition zone (ITZ). At 8 % MK, flexure improves to 14.25 MPa (+3.6 % over 7 % MK, +11.8 % over 6 % MK, and +1.8 % above the control) showing that once workability is adequate, MK's ultrafine filler effect and rapid aluminosilicate reaction strengthen tensile load paths and crack-arresting bridges. For downstream fracture or fatigue tests, this matters: MK near 8 % should widen the stable microcrack regime and delay first-crack formation, yielding higher modulus of rupture scatter resistance. Conversely, the 6 % MK data warn that under-dosed superplasticizer or suboptimal paste

volume can mask MK's chemical benefits by weakening compaction and the ITZ [28]. If you plan to compare toughness or flexural fatigue across binders, keep slump consistent and use MK 7–8 % as the reference region; it maximizes ITZ refinement without excessive dilution of clinker. These trends suggest that modest MK additions primarily enhance matrix continuity rather than just compressive capacity, which is crucial when bending governs performance (e.g., slabs, pavements, thin precast elements).

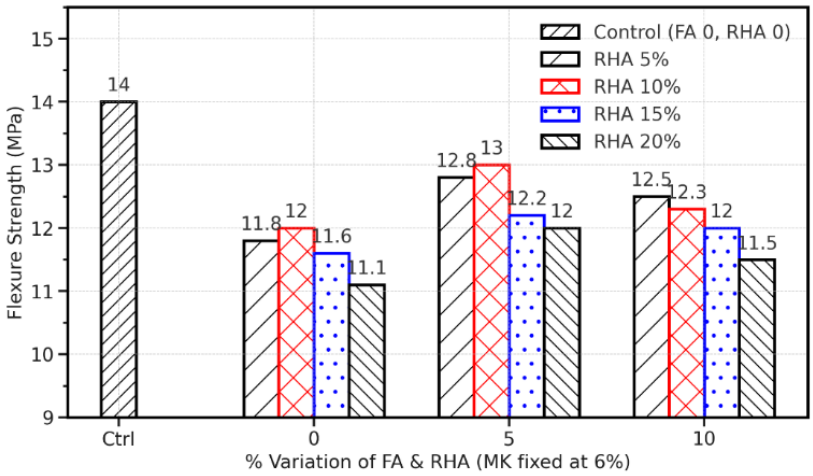

Figure 10. Typical results for flexure strength of ternary blended concrete mixes at 28 days curing.

Fig. 10 depicts the advancement of flexural strength in concrete mixtures incorporating various cement replacement ingredients, specifically 6 % MK, 5–15 % FA, and 5–20 % RHA. An experiment was conducted to investigate the effect of varying RHA percentages on the flexural strength of concrete. The concrete mixture comprised a constant composition of 6 % MK and 5 % FA. The results indicated a significant enhancement in flexural strength after 28 days of curing with the addition of 10 % RHA (M3). This rise parallels the trend noted when combining alone with 6 % MK. Further investigation indicates similar variations for 10 and 15 % FA, alongside a range of 5–20 % RHA and 6 % MK. Following a 28-day curing period, it was observed that the formulation designated as M7, comprising 74 % OPC, 6 % MK, 10 % FA, and 10% RHA, exhibited marginally inferior flexural strength relative to the control mixture (M0). The conclusion reached is illustrated in Fig. 10. The predominance of FA's behavior is evident in the M6–M9 mix, especially in contrast to the M2–M5 mix, particularly with the addition of 10 % FA. The ideal blending combination that produces the highest flexural Strength for all mixes is identified as 8 % MK + 10 % FA + 10 % RHA (designated M33) for ternary blending, and 8 % MK (designated M27) for single blending [29].

Split tensile strength

The mean split tensile strength of concrete specimens, assessed after 28 days of water curing, is recorded. Fig. 11 shows the split tensile strength response as MK replaces cement from 0 to 8 %. The control (0 % MK) records 2.44 MPa. Introducing 6 % MK reduces the strength to 2.27 MPa, a 7.0 % drop, consistent with the higher specific surface area of MK, which raises water and superplasticizer demand. If the admixture dosage is not adjusted, compaction efficacy and ITZ quality suffer, which depresses the tensile capacity. Increasing MK to 7 % lifts strength to 2.41 MPa (+6.2 % vs 6 % MK; −1.2 % vs control), suggesting improved particle packing and early pozzolanic refinement that stabilizes microcrack initiation. At 8 % MK, strength reaches 2.47 MPa (+8.8 % relative to 6 % MK and +1.2 % above the control) indicating that once slump is managed, MK's ultrafine filler and reactive aluminosilicate gels densify the ITZ and enhance crack-bridging paths under diametral loading. Practically, the 6 % MK dip signals sensitivity to rheology; maintaining constant workability across mixes is critical so tensile results reflect binder chemistry rather than casting artifacts. For fracture energy, permeability, or chloride tests that are strongly influenced by microcrack networks, an MK near 7–8 % is a useful setting: it slightly increases tensile strength while also promoting a tighter pore structure, which should reduce connected capillaries. If your study explores synergy with FA/RHA, use MK 8 % as the tensile-strength benchmark and adjust superplasticizer to match control slump; this will help prevent porosity differences from skewing strength, transport, or durability outcomes [30].

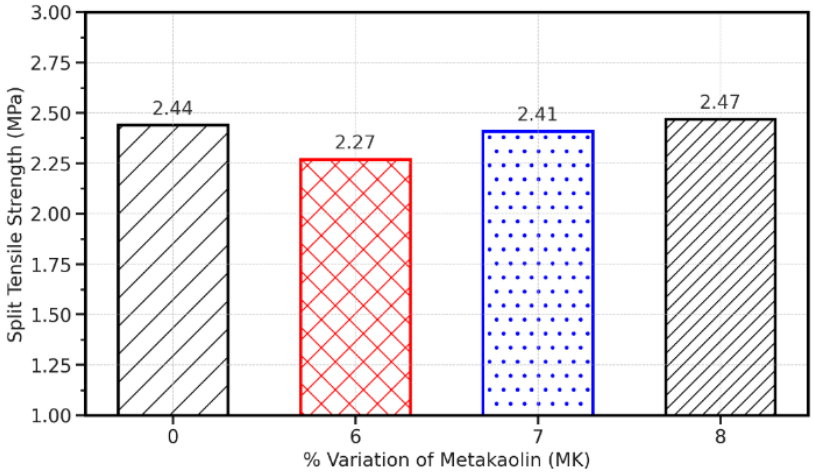

Figure 11. Split tensile strength of ternary blended concrete mixes using 6–8 % MK only.

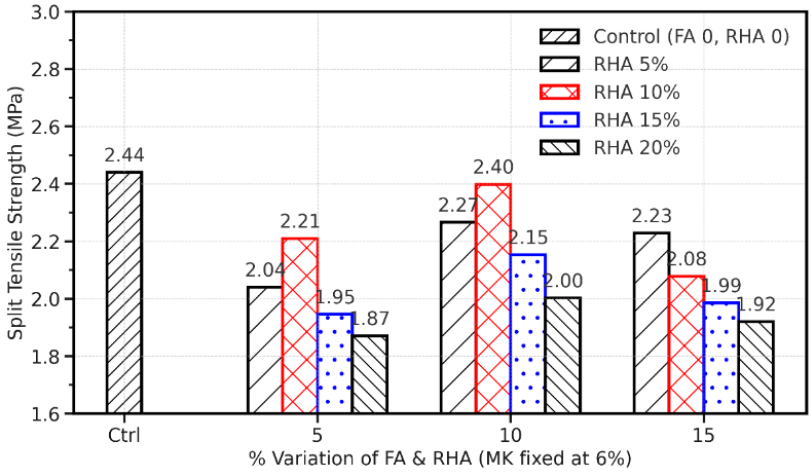

Figure 12. Typical results for split tensile strength of ternary blended concrete mixes at 28 days curing.

Fig. 12 illustrates the standard outcomes of split tensile strength progression in ternary blended concrete mixtures. These combinations consist of substituting a designated quantity of cement with 6 % MK, 5–15 % FA, and 5–20 % RHA, along with one control mixture. The results depicted in Fig. 12 indicate a significant increase in the split tensile strength of concrete with the addition of varying quantities of RHA to a constant mixture comprising 6 % MK and 5 % FA. A notable enhancement in split tensile strength is observed when 10 % RHA (designated as M3) is incorporated into the concrete, with a 28-day curing duration. Subsequent analysis reveals analogous fluctuations for 10 and 15 % FA in relation to the range of 5–20 % RHA and 6 % MK. Furthermore, the influence of FA is more pronounced in combinations M6–M9 than in mixtures M2–M5, particularly when FA is integrated at a 10 % level [31].

According to the results illustrated in Fig. 12, the M10 mixes demonstrate superior values compared to the M11–M13 mixes. Nonetheless, they remain inferior to both the control mixture and the other combinations employed for M6–M9. Fig. 12 illustrates that the strength values improve when the FA concentration rises from 5 to 10 %. Nonetheless, a shift in tendency occurs from M10–M13 as the FA percentage increases from 10 to 15 %. The findings clearly indicate that the ideal proportion of FA for these mixtures is 10 %. According to Fig. 12, the optimal outcome is achieved by employing a combination of all chemicals, particularly 6 % MK, 10 % FA, and 10 % RHA. The incorporation of MK in plain cement concrete resulted in a minor reduction in split tensile strength, however the decrease was not substantial. Consequently, thorough study reveals that the optimal formulation for attaining maximum split tensile strength across all mixtures is a combination of 8 % MK, 10 % FA, and 10 % RHA (designated as M33) for ternary blending, and 8 % MK (designated as M27) for single blending.

3.4. Proposed Approach for the Combined Effect (Synergy) of Mineral Admixtures

The term “synergistic impact” denotes the interaction of two or more substances that results in a combined effect beyond the cumulative effects of the individual substances. Prior research has shown that

the synergistic effect and efficiency factor of MK are superior in binary cement concrete compared to analogous single blended cement concrete. This applies when contrasting the two compounds. These data suggest that the efficiency factor of MK is superior in a ternary blending system of concrete mixes compared to the efficiency factor observed in binary or single blending cement concrete.

A formula has been presented to ascertain the efficiency factor of MK, FA, and RHA in ternary cement concrete. This formula, as elucidated by researchers, is derived from Bolomey's equation, which is used to estimate the strength of concrete incorporating mineral admixtures. The water-to-cement ratio has been maintained at a constant value of 0.45 during the entire experimental research. Bolomey's equation can be utilized to forecast the compressive strength of the control mix:

$$f_c\left(days\right) = A_1\left(C/W\right) + A_2, \tag{1}$$

where f_c is the anticipated compressive strength; A_1 and A_2 are the constants that take into consideration the varying ages of concrete; C is the amount of cement, kg/m^3; W is the amount of water present per unit volume, kg/m^3.

In (1), the constants A_1 and A_2 have been included to account for various factors, such as the age of the concrete and exposure conditions, that may influence the development of the concrete's strength. These parameters can be determined by regression analysis. The concrete's strength was previously determined in research by examining the precise effects of admixtures on its chemical composition. This was achieved by altering Bolomey's equation, as seen in (2) [32]:

$$f_c\left(days\right) = A_1\left\{\left(C + k_{MA}P_{MA}\right)/W\right\} + A_2. \tag{2}$$

In the context of concrete mixes, k_{MA} refers to the efficiency factor of the mineral addition that is utilized, while P_{MA} reflects the amount of mineral admixture, kg/m^3. In addition, the efficiency factor k_{MA} has been calculated using (3), as provided by the researchers:

$$k_{MA} = \left(1/P_{MA}\right)\left\{-C + W\left(f_c - A_2\right)/A_1\right\}. \tag{3}$$

After calculating the individual effect $\left(k_{MA}\right)$, it is important to determine the combined effect, known as the synergy, of this mineral admixture. This synergy or combined effect of two or more additives are used, which is represented as k_{TB}, which is a factor that represents the combined effect of the mineral admixture in binary, ternary, or quaternary cement concrete. The value of k_{TB} is predicted using the following equation:

$$k_{TB} = \left\{W\left(f_c - A_2\right)/A_1 - C\right\}/\left(k_{MA}P_{MA}\right). \tag{4}$$

As a result, the overall efficiency factor for mineral admixture $\left(k'_{MA}\right)$ is calculated by taking into consideration the combined effect of all of the admixtures that are utilized in the concrete mixes. The value was determined by applying (5) to the data:

$$k'_{MA} = k_{TB} \times k_{MA}. \tag{5}$$

The symbol *k* denotes the final efficiency factor of mineral admixture in binary cement concrete. With the use of the following connection, a formula has been developed to estimate the compressive strength of binary cement concrete. The formula is as follows:

$$f_c\left(days\right) = A_1\left\{C/W + k_{TB}\left(k_{MA}P_{MA}\right)/W\right\} + A_2, \tag{6}$$

where f_c is the predicted compressive strength; A_1 and A_2 are the constants that take into account the varying ages of the concrete; C is the cement content, kg/m^3; W is the water content, kg/m^3, k_{TB} is the synergic impact factor of mineral admixture; k_{MA} is the efficiency factor of mineral admixture; P_{MA} is the mineral admixture content, kg/m^3.

It is important to note that the equation presented above only displays compressive strength values for cement blends that contain only two components. Consequently, the equation that was presented earlier

can also be extended to include ternary or quaternary cement concrete conditions. The equation for ternary concrete (7) can be produced by carrying out the aforementioned steps. In a similar manner, it is possible to develop an equation for quaternary concrete, which is represented by (8):

$$f_c\left(days\right)=A_1\left\{C/W+k_{TB}\left(k_{MA_1}P_{MA_1}+k_{MA_2}P_{MA_2}\right)/W\right\}+A_2; \tag{7}$$

$$f_c\left(days\right)=A_1\left\{C/W+k_{TB}\left(k_{MA_1}P_{MA_1}+k_{MA_2}P_{MA_2}+k_{MA_3}P_{MA_3}\right)/W\right\}+A_2. \tag{8}$$

The variables k_{MA_1}, k_{MA_2}, and k_{MA_3} represent the efficiency factors for mineral admixture types 1, 2, and 3, respectively. The variables P_{MA_1}, P_{MA_2}, and P_{MA_3} represent the content of mineral admixture types 1, 2, and 3, respectively.

However, in this particular investigation, the identical equation form for f_c (8) has been utilized for predictive purposes. However, new coefficient terms have been substituted for k_{TB} and k_{MA_1}, k_{MA_2} and k_{MA_3}. There were three different types of admixtures used in the research: MK, FA, and RHA. According to the equation, the coefficients that are allocated to each admixture are denoted by the symbols α_{MK}, α_{FA}, and α_{RHA}. These coefficients can be considered analogous to the efficiency factors of MK, FA, and RHA, denoted as k_{MK}, k_{FA}, and k_{RHA}, respectively. It is also worth noting that k_{TB} is considered equivalent to α_{TB}.

$$f_c\left(days\right)=A_1\left\{C/W+\alpha_{TB}\left(\alpha_{MK}P_{MK}+\alpha_{FA}P_{FA}+\alpha_{RHA}P_{RHA}\right)/W\right\}+A_2. \tag{9}$$

The terms α_{MK}, α_{FA}, and α_{RHA} correspond to the efficiency factors of MK, FA, and RHA, respectively. Additionally, α_{TB} is the factor that corresponds to the factor that shows how all of the admixtures in ternary blended concrete mixes work together synergistically. As a result, the final proposed equation (9) is used in the same way as described earlier and serves as an analogy for (8).

The overall efficiency factor for each admixture, represented as k'_{MA}, is calculated by assessing the collective impact of all the admixtures employed in the concrete mixes, as outlined in (5). In this study, the component is represented as α'_{MK}, which can be seen as comparable to k'_{MK}. The value has been calculated using the equation $\alpha'_{MK}=\alpha_{TB}\times\alpha_{MK}$, where α'_{MK} represents a comparable parameter to the final efficiency factor of MK (i.e., k'_{MK}). Therefore, (5) may also be used to generate analogous derivations for FA and RHA.

Equation (9) can be used in nonlinear regression analysis to predict the efficiency factor for numerous mineral admixtures simultaneously. The subsequent procedures have been executed to predict the collective influence and the related coefficients of MK, FA, and RHA for ternary blended concrete mixes:

Step 1: A_1 and A_2 are constants that represent the varying ages of concrete. These constants were determined by regression analysis using (9), as displayed in Table 6.

Table 6. A_1 and A_2 at different ages of concrete.

Age of Concrete (days)	A_1	A_2
7	9.79	1.41
28	10.88	24.29
56	11.43	30.55

Step 2: The coefficients α_{MK}, α_{FA}, and α_{RHA}, which represent the equivalent properties of MK, FA, and RHA in ternary blended concrete mixes at various ages, were computed using (9). The calculated coefficients are presented in Table 7.

Table 7. Analogous coefficient of MK, FA and RHA in ternary blended concrete.

Age of Concrete (days)	α_{MK}	α_{FA}	α_{RHA}
7	1.06	0.63	–0.20
28	1.71	1.09	–3.93
56	1.84	1.11	–4.62

Step 3: The synergistic impact factor of additives (α_{TB}) was determined using (9) for various combinations of ternary blended concrete, as presented in Table 8.

Table 8. Synergic effect factor of all admixtures in ternary blended concrete.

Age of Concrete (days)	α_{TB}
7	1.97
28	2.14
56	2.88

Step 4: Table 9 contains the comparable parameter to the final efficiency factor of all additions in ternary blended concrete mixes.

Table 9. Analogous parameter to the final efficiency factor of all admixtures in ternary blended concrete.

Age of Concrete (days)	$\alpha'_{MK} = \alpha_{TB} \times \alpha_{MK}$	$\alpha'_{FA} = \alpha_{TB} \times \alpha_{FA}$	$\alpha'_{RHA} = \alpha_{TB} \times \alpha_{RHA}$
7	2.08	1.24	–0.39
28	3.65	2.33	–8.41
56	5.29	3.19	–13.30

The rate of increase in the final efficiency factor of all admixtures is continually rising for concrete of all ages. Nevertheless, the deviation in parameters for concrete at 28 and 56 days is negligible in comparison to the fluctuation in parameters for admixtures at 7 and 28 days.

3.5. Estimating the Compressive Strength of Concrete Using Ternary Blending

The compressive strength of various ternary blending concrete mixes in this investigation can be determined using the following formulae:

$$f_c\left(7\ days\right) = 9.79\left\{C/W + 1.97\left(\left(1.06\right)P_{MK} + \left(0.63\right)P_{FA} + \left(-0.20\right)P_{RHA}\right)/W\right\} + 1.41; \quad (10)$$

$$f_c\left(28\ days\right) = 10.88\left\{C/W + 2.14\left(\left(1.71\right)P_{MK} + \left(1.09\right)P_{FA} + \left(-3.93\right)P_{RHA}\right)/W\right\} + 24.29; \quad (11)$$

$$f_c\left(56\ days\right) = 2.55\left\{C/W + 2.88\left(\left(1.84\right)P_{MK} + \left(1.11\right)P_{FA} + \left(-4.62\right)P_{RHA}\right)/W\right\} + 34.62. \quad (12)$$

Figs. 13–15 display the comparison between the experimental and projected values of compressive strength at 7, 28, and 56 days, respectively.

Fig. 13 illustrates the regression equation obtained with the MS Excel application utilizing the Solver function. This equation is utilized to create a graph that juxtaposes the experimental results with the expected values of compressive strength at 7 days. Of the 40 data sets, 10 sets, including 25 % of the total, have forecast errors exceeding 10 %. The remaining 30 sets, including 75 % of the total, exhibit an enhancement in inaccuracy within the range of 0–10 %.

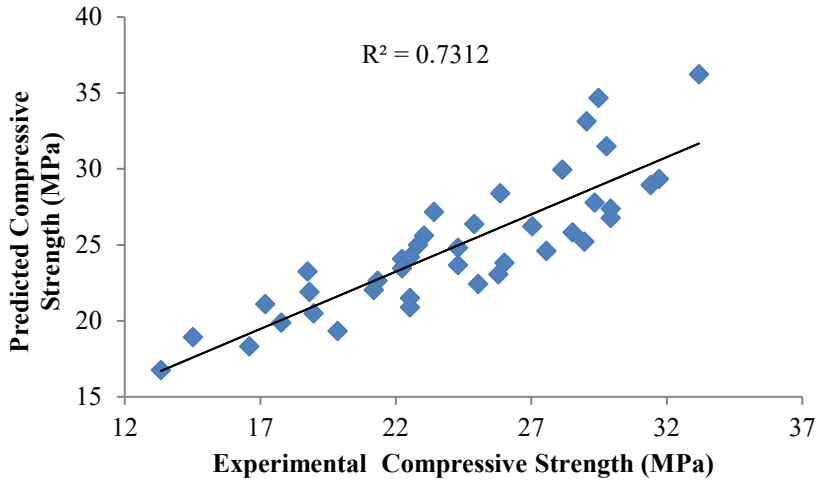

Figure 13. Comparison between experimental vs. predicted values at 7 days.

Fig. 14 illustrates the regression equation produced by the MS Excel application with the solver function. This equation is used to create a graph that compares the measured and projected values of compressive strength after 28 days. Out of 40 data sets, 30 % (12 sets) exhibit an error exceeding 10 %, whilst the remaining 70 % (28 sets) demonstrate a decrease in error, ranging from 0 to 10 %.

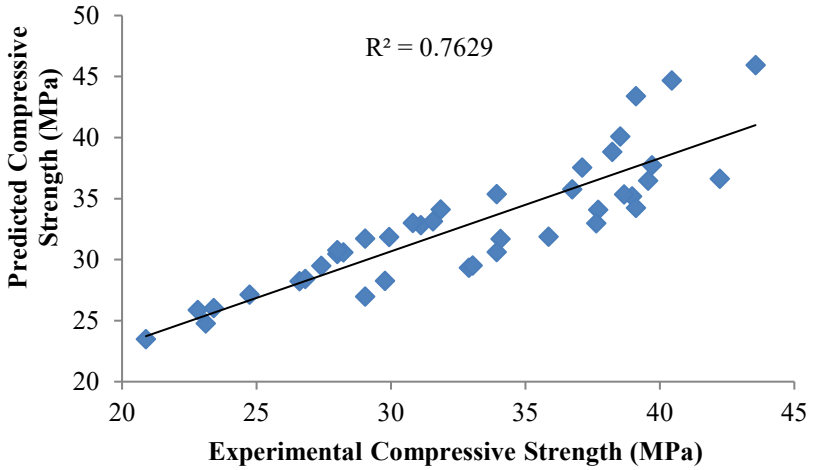

Figure 14. Comparison between experimental vs. predicted values at 28 days.

Fig. 15 illustrates the regression equation generated by the MS Excel application using the Solver function. This equation is employed to illustrate a graphical comparison between the actual experimental data and the anticipated values of compressive strength after 56 days. Of the 40 data sets, 20 % (8 sets) exhibit forecast errors exceeding 10 %, whilst the remaining 80 % (32 sets) demonstrate error reductions within the 0–10 % range.

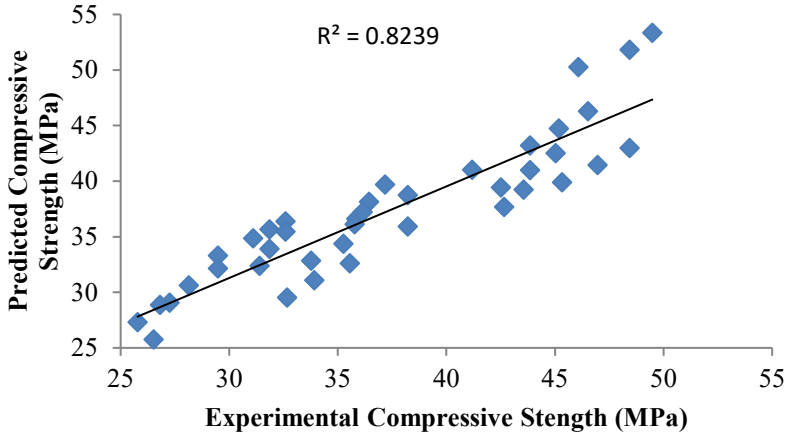

Figure 15. Comparison between experimental vs. predicted values at 56 days.

The observed disparity indicates a substantial correlation between the actual results and the expected data. The error variation appears to be within an acceptable range, since over 80 % of the data exhibits substantial concordance with the testing results. The R^2 values for maturity periods of 7, 28, and 56 days are 0.73, 0.76, and 0.82, respectively, as illustrated in Figs. 13–15. Despite the low results, the link may still be established by examining the variation in errors. The comparatively low value of R^2 can be attributed to the principle of analogy.

3.6. Correlation between Compressive Strength and Split Tensile Strength

Regression analysis was employed to establish the link between split tensile strength and compressive strength. The compressive strength of the specimens was determined by measuring the resistance to compression using cubic samples with dimensions of 150×150×150 mm. The split tensile strength was determined by measuring the resistance to splitting using cylindrical samples with dimensions of 75×150 mm after a 28-day period. By utilizing regression analysis with the provided equations, we may examine the present strength data of all concrete mixes and ascertain the most suitable curve that fits the data.

Following expression has been adopted with a confidence level of good predictions.

$$f_t = \left[x_1 \times \left(f_c \right)^{x_2} \right] - x_3.$$

In this context, the constants x_1, x_2, and x_3 are determined through the utilization of Non-Linear Regression analytical techniques. The values of the constants obtained are: x_1 = 5.31, x_2 = 0.14, x_3 = 6.51. In light of this, the empirical equation can be written as:

$$f_t = \left[5.31 \times f_c^{0.14} \right] - 6.51, \quad (13)$$

where f_t is equal to the split tensile strength, MPa; f_c equals the compressive strength, MPa.

Due to concrete's greater levels of uncertainty compared to other materials, the equation yields an underestimated result, which is practically logical. Consequently, it is preferable to formulate an equation that yields a result inferior to the anticipated one. Out of the forty data sets, eight sets (20 %) demonstrate forecast errors above 10 %, whereas the remaining thirty-one sets (80 %) indicate error reductions ranging from 0 to 10 %. However, discrepancies in the expected outcomes may arise from the unpredictability and dispersion of the experimental data set. The correlation may be validated by examining the error variability in the projected data, which clearly demonstrates a high level of confidence in the predicted values and facilitates the alignment of results with the experimental data. Fig. 16, which illustrates a dataset with an error margin of ±10 %, has been included for clarity.

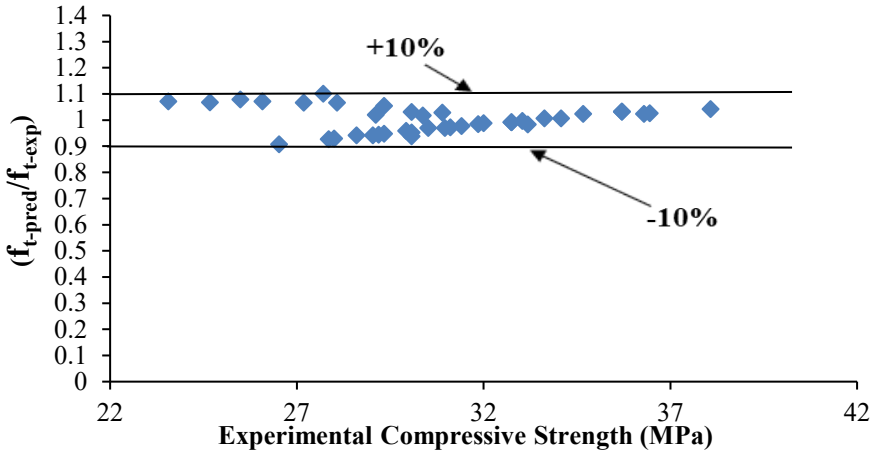

Figure 16. Error variation of predicted vs experimental values of split tensile strength.

3.7. Correlation between Compressive Strength and Flexure Strength

A regression analysis was performed to establish the degree of correlation between flexural strength and compressive strength. As part of the research, cubes measuring 150×150×150 mm were utilized to evaluate the compressive strength of the material. Additionally, beams measuring 100×100×500 mm were utilized to measure the flexural strength after a period of 28 days:

Following expression has been adopted with a confidence level of good predictions.

$$f_b = \left[x_1 \times \left(f_c \right)^{x_2} \right] / x_3 .$$

The values of constants x_1, x_2, and x_3 are determined by the use of nonlinear regression analysis. The values acquired for the aforementioned constants are: x_1 = 0.85, x_2 = 0.68, x_3 = 0.77. Hence the final expression is formed as:

$$f_b = \left[\left[0.85 \times \left(f_c \right)^{0.68} \right] / 0.77 \right], \quad (14)$$

where f_b represents the flexure strength, MPa; f_c represents the compressive strength of a material, MPa.

Out of the 40 data sets, 6 sets (15 %) exhibit forecast errors over 10 %, whereas the remaining 34 sets (85 %) have errors below 10 %, specifically within the range of 0 to 10 %. However, discrepancies in the expected outcomes may arise from the unpredictability and dispersion of the experimental data set. The correlation can be validated by examining the error variability in the projected data, which clearly demonstrates the reliability of the predicted values and facilitates the alignment of results with the experimental data. Nonetheless, Fig. 17, which depicts a dataset with a ±10 % margin of error, has been included here to enhance comprehension.

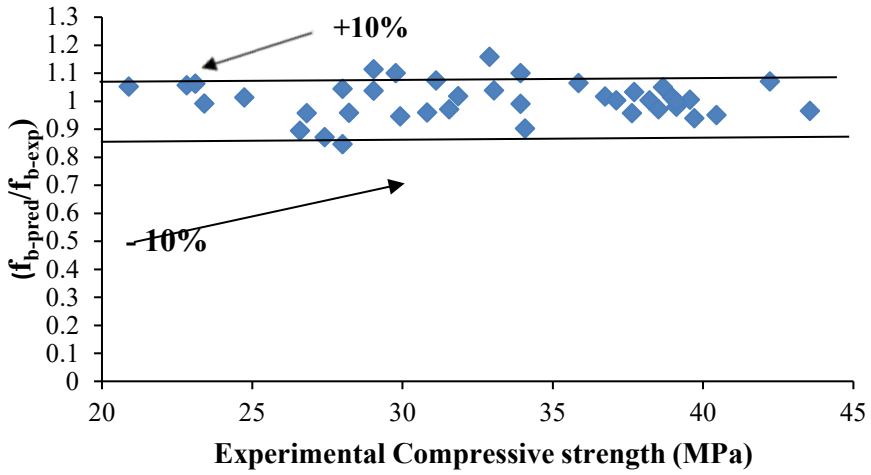

Figure 17. Error variation of predicted vs experimental values of flexure strength.

4. Conclusion

This work has shown that ternary mineral admixtures can reduce clinker while preserving structural performance when proportioned with attention to rheology and late-age reactions. Slump had decreased as fines increased: raising MK from 0 to 8 % reduced slump from 188 to 172 mm (−8.5 %), and at MK 6 % the combinations FA 0/RHA 20 %, FA 10 %/RHA 20 %, and FA 15 %/RHA 20 % had yielded 67, 44, and 35 mm, respectively, which had indicated strong water and superplasticizer demand. Strength responses had mapped a clear hierarchy. MK alone at 8 % produced 30.10 MPa at 7 days, 37.20 MPa at 28 days, and 41.76 MPa at 56 days, surpassing the 100 % OPC control at both 28 and 56 days. The most effective ternary blend across the 39 mixtures was MK 8 % + FA 10 % + RHA 10 %, reaching approximately 30.9 MPa at 7 days, 38.9 MPa at 28 days, and 42.6 MPa at 56 days. At the same MK level, pushing RHA beyond 10 % had depressed 28-day strength to 31.3 MPa at 15 % RHA and 28.8 MPa at 20 % RHA, with 56-day values of 33.99 and 32.06 MPa, respectively. This confirms that excessive porous silica had diluted the clinker and increased admixture adsorption. Tensile responses were sensitive but recoverable: with MK 6 %, the mix FA 10 %/RHA 10 % had reached 2.40 MPa in splitting, compared with 2.44 MPa for the control. Meanwhile, MK 8 % alone had increased flexural strength to 14.25 MPa, compared with 14.00 MPa for the control. The synergy-based equations had predicted compressive strength across the matrix and had supported conversion to split-tensile and flexural values, providing a design-ready pathway for clinker reduction. The findings supported an MK near 8 % with FA and RHA at about 10 % each, coupled with admixture retuning to maintain the target slump, as a practical recipe for strength retention. Future work is encouraged to quantify permeability, chloride ingress and freeze-thaw resistance for the recommended

blends, to couple rheology measurements with admixture chemistry for reliable placement at low w/b ratios, and to validate the predictive framework using multi-source materials and field-cast elements.

References

1. Das, M., Adhikary, S.K., Rudžionis, Ž. Effectiveness of fly ash, zeolite, and unburnt rice husk as a substitute of cement in concrete. Materials Today: Proceedings. 2022. 61(2). Pp. 237–242. DOI: 10.1016/j.matpr.2021.09.005
2. Bui, P.-T., Huynh, T.-P. Performance and microstructural evaluation of rice husk ash-ground granulated blast furnace slag-CFBC fly ash mixtures produced as an eco-cement. Journal of Materials in Civil Engineering. 2022. 34(3). Article no. 04021485. DOI: 10.1061/(ASCE)MT.1943-5533.0004119
3. Chindaprasirt, P., Rukzon, S. Pore structure changes of blended cement pastes containing fly ash, rice husk ash, and palm oil fuel ash caused by carbonation. Journal of Materials in Civil Engineering. 2009. 21(11). Pp. 666–671. DOI: 10.1061/(ASCE)0899-1561(2009)21:11(666)
4. Alrowaili, Z.A., Alnairi, M.M., Olarinoye, O.I., Alhamazani, A., Alshammari, G.S., Al-Buriahi, M.S. Radiation attenuation of fly ash and rice husk ash-based geopolymers as cement replacement in concrete for shielding applications. Radiation Physics and Chemistry. 2024. 217. Article no. 111489. DOI: 10.1016/j.radphyschem.2023.111489
5. Kuffner, B.H.B., Tambara Jr., L.U.D., Marangon, E, Lübeck, A. Development of self-compacting concretes using rice husk or fly ashes and different cement types. REM – International Engineering Journal. 2023. 76(1). Pp. 9–19. DOI: 10.1590/0370-44672021760007
6. Kathirvel, P., Saraswathy, V., Karthik, S.P., Sekar, A.S.S. Strength and durability properties of quaternary cement concrete made with fly ash, rice husk ash and limestone powder. Arabian Journal for Science and Engineering, 2013. 38. Pp. 589–598. DOI: 10.1007/s13369-012-0331-1
7. Öztürk, M., Karaaslan, M., Akgöl, O., Sevim, U.K. Mechanical and electromagnetic performance of cement based composites containing different replacement levels of ground granulated blast furnace slag, fly ash, silica fume and rice husk ash. Cement and Concrete Research. 2020. 136. Article no. 106177. DOI: 10.1016/j.cemconres.2020.106177
8. Vijaya, S.K., Jagadeeswari, K., Karri, S. Behaviour of M60 grade concrete by partial replacement of cement with fly ash, rice husk ash and silica fume. Materials Today: Proceedings, 2021. 37(2). Pp. 2104–2108. DOI: 10.1016/j.matpr.2020.07.523
9. Subramaniam, D.N., Sathiparan, N. Comparative study of fly ash and rice husk ash as cement replacement in pervious concrete: mechanical characteristics and sustainability analysis. International Journal of Pavement Engineering. 2023. 24(2). Article no. 2075867. DOI: 10.1080/10298436.2022.2075867
10. Darsanasiri, A.G.N.D., Matalkah, F., Ramli, S., Al-Jalode, K., Balachandra, A., Soroushian, P. Ternary alkali aluminosilicate cement based on rice husk ash, slag and coal fly ash. Journal of Building Engineering. 2018. 19. Pp. 36–41. DOI: 10.1016/j.jobe.2018.04.020
11. Ouypornprasert, W., Traitruengtatsana, N., Kamollertvara, K. Optimum Partial Replacement of Cement by Rice Husk Ash and Fly Ash Based on Complete Consumption of Calcium Hydroxide. Materials for Sustainable Infrastructure. GeoMEast 2017. Sustainable Civil Infrastructures. Springer. Cham, 2018. Pp. 145–184. DOI: 10.1007/978-3-319-61633-9_10
12. Chindaprasirt, P., Kanchanda, P., Sathonsaowaphak, A., Cao, H.T. Sulfate resistance of blended cements containing fly ash and rice husk ash. Construction and Building Materials. 2007. 21(6). Pp. 1356–1361. DOI: 10.1016/j.conbuildmat.2005.10.005
13. Payá, J., Monzó, J., Borrachero, M.V., Amahjour, F., Girbés, I., Velazquez, S., Ordóñez, L.M. Advantages in the use of fly ashes in cements containing pozzolanic combustion residues: silica fume, sewage sludge ash, spent fluidized bed catalyst and rice husk ash. Journal of Chemical Technology and Biotechnology. 2002. 77(3). Pp. 331–335. DOI: 10.1002/jctb.583
14. Chindaprasirt, P., Rukzon, S. Strength, porosity and corrosion resistance of ternary blend Portland cement, rice husk ash and fly ash mortar. Construction and Building Materials. 2008. 22(8). Pp. 1601–1606. DOI: 10.1016/j.conbuildmat.2007.06.010
15. Fernando, S., Gunasekara, C., Law, D.W., Nasvi, M.C.M., Setunge, S. Development of Blended Fly Ash-Rice Husk Ash–Based Alkali-Activated Bricks: A Sustainable Alternative to Portland Cement Brick. Lecture Notes in Civil Engineering. 2023. 266: 12th International Conference on Structural Engineering and Construction Management. Pp. 643–653. DOI: 10.1007/978-981-19-2886-4_45
16. Chindaprasirt, P., Rukzon, S., Sirivivatnanon, V. Resistance to chloride penetration of blended Portland cement mortar containing palm oil fuel ash, rice husk ash and fly ash. Construction and Building Materials. 2008. 22(5). Pp. 932–938. DOI: 10.1016/j.conbuildmat.2006.12.001
17. Muthanand, P., Nagarajan, M., Sarathbabu, M. Experimental study on rice husk ash and fly ash as partial replacement of cement in concrete. International Journal of Civil Engineering and Technology. 2018. 9(11). Pp. 1170–1177.
18. Karim, M.R., Zain, M.F.M., Jamil, M., Lai, F.C. Development of a zero-cement binder using slag, fly ash, and rice husk ash with chemical activator. Advances in Materials Science and Engineering. 2015. 2015. Article no. 247065. DOI: 10.1155/2015/247065
19. Bhanumathidas, N., Mehta, P.K. Concrete mixtures made with ternary blended cements containing fly ash and rice-husk ash. Seventh CANMET/ACI International Conference on Fly Ash, Silica Fume, Slag and Natural Pozzolans in Concrete. American Concrete Institute. Farmington Hills, MI, 2001. Pp. 379–391.
20. Behnood, A., Modiri Gharehveran, M., Gozali Asl, F., Ameri, M. Effects of copper slag and recycled concrete aggregate on the properties of CIR mixes with bitumen emulsion, rice husk ash, Portland cement and fly ash. Construction and Building Materials. 2015. 96. Pp. 172–180. DOI: 10.1016/j.conbuildmat.2015.08.021
21. Medina, C., Sáez del Bosque, I.F., Frías, M., Sánchez de Rojas, M.I. Design and characterisation of ternary cements containing rice husk ash and fly ash. Construction and Building Materials. 2018. 187. Pp. 65–76. DOI: 10.1016/j.conbuildmat.2018.07.174
22. Kanthe, V.N., Deo, S.V., Murmu, M. Effect of fly ash and rice husk ash on strength and durability of binary and ternary blend cement mortar. Asian Journal of Civil Engineering. 2018. 19. Pp. 963–970. DOI: 10.1007/s42107-018-0076-6
23. Kanthe, V.N., Deo, S.V., Murmu, M. Effect of fly ash and rice husk ash as partial replacement of cement on packing density and properties of cement. International Journal of Innovative Technology and Exploring Engineering (IJITEE). 2019. 8(7). Pp. 1940–1945.
24. Hou, Y., Yin, S., Wang, L., Zheng, K., Yang, K., Wang, Y. Mechanical properties, microstructure and parameter optimization of fly ash-rice husk ash cement backfill. China Mining Magazine. 2025. 34(8). Pp. 178–189. DOI: 10.12075/j.issn.1004-4051.20241972

25. Sathawane, S.H., Vairagade, V.S., Kene, K.S. Combine Effect of Rice Husk Ash and Fly Ash on Concrete by 30% Cement Replacement. Procedia Engineering. 2013. 51. Pp. 35–44. DOI: 10.1016/j.proeng.2013.01.009
26. Fernando, S., Gunasekara, C., Law, D.W., Nasvi, M.C.M., Setunge, S., Dissanayake, R. Engineering properties of waste-based alkali activated concrete brick containing low calcium fly ash and rice husk ash: A comparison with traditional Portland cement concrete brick. Journal of Building Engineering. 2022. 46. Article no. 103810. DOI: 10.1016/j.jobe.2021.103810
27. Khalil, N.M., Hassan, E.M., Shakdofa, M.M.E., Farahat, M. Beneficiation of the huge waste quantities of barley and rice husks as well as coal fly ashes as additives for Portland cement. Journal of Industrial and Engineering Chemistry. 2014. 20(5). Pp. 2998–3008. DOI: 10.1016/j.jiec.2013.11.034
28. Sukkarak, R., Thangjaroensuk, B., Kongkitkul, W., Jongpradist, P. Strength and Equivalent Modulus of Cement Stabilized Lateritic with Partial Replacement by Fly Ash and Rice Husk Ash. Engineering Journal. 2021. 25(10). Pp. 13–25. DOI: 10.4186/ej.2021.25.10.13
29. Krishna, P.U.S., Reddy, K.R., Devi, L.I., RadhaKrishna, V., Kumar, D.P. Experimental Investigation on the Strengths of Cement Bricks Using Fly Ash and Rice Husk Wastes: Recycling Waste Materials. Innovations in Energy Efficient Construction Through Sustainable Materials. IGI Global Scientific Publishing, 2025. Pp. 83–106. DOI: 10.4018/979-8-3693-3398-3.ch004
30. Subramaniam, D.N., Sathiparan, N. Correction (Comparative study of fly ash and rice husk ash as cement replacement in pervious concrete: mechanical characteristics and sustainability analysis). International Journal of Pavement Engineering. 2023. 24(2). Article no. 2148067. DOI: 10.1080/10298436.2022.2148067
31. Rukzon, S., Chindaprasirt, P. Mathematical model of strength and porosity of ternary blend Portland rice husk ash and fly ash cement mortar. Computers and Concrete. 2008. 5(1). Pp. 75–88. DOI: 10.12989/cac.2008.5.1.075
32. Sukkarak, R., Thangjaroensuk, B., Jongpradist, P. Evaluation of fly ash and rice husk ash on the unconfined compressive strength of the compacted cement treated lateritic soil. Suranaree Journal of Science and Technology. 2022. 29(5). Article no. 010169.

Information about the authors:

Ashok Kumar,
E-mail: ashokkumar.civil@nitjsr.ac.in

Virendra Kumar,
E-mail: virendrakumar.ce@nitjsr.ac.in

Sanjay Kumar,
E-mail: sanjaykumar.civil@nitjsr.ac.in

Alexandr Orlov,
E-mail: orlovak@mgsu.ru

Saurav Dixit, *PhD*
E-mail: sauravarambol@gmail.com

Received: 06.01.2025. Approved: 10.09.2025. Accepted: 11.09.2025.